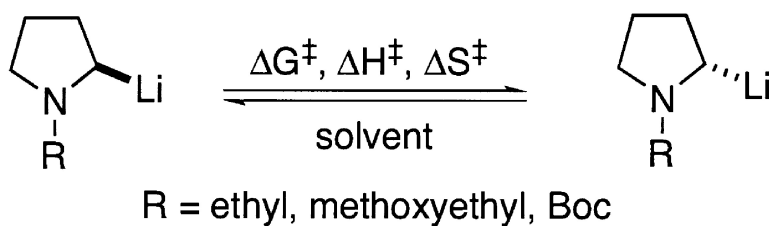


Barrier to Enantiomerization of Unstabilized, Chelated, and Dipole-Stabilized 2-Lithiopyrrolidines

Neil J. Ashweek, Peter Brandt, Iain Coldham, Samuel Dufour,
 Robert E. Gawley, , Rosalyn Klein, and Graciela Sanchez-Jimenez

J. Am. Chem. Soc., **2005**, 127 (1), 449-457 • DOI: 10.1021/ja048090I • Publication Date (Web): 04 December 2004

Downloaded from <http://pubs.acs.org> on March 24, 2009



More About This Article

Additional resources and features associated with this article are available within the HTML version:

- Supporting Information
- Links to the 3 articles that cite this article, as of the time of this article download
- Access to high resolution figures
- Links to articles and content related to this article
- Copyright permission to reproduce figures and/or text from this article

[View the Full Text HTML](#)

Barrier to Enantiomerization of Unstabilized, Chelated, and Dipole-Stabilized 2-Lithiopyrrolidines

Neil J. Ashweek,[†] Peter Brandt,[‡] Iain Coldham,^{*,†,§} Samuel Dufour,[†]
Robert E. Gawley,^{*,¶,#} Fredrik Hæffner,^{*,@} Rosalyn Klein,^{¶,#} and
Graciela Sanchez-Jimenez[§]

Contribution from the Department of Chemistry, University of Exeter, Stocker Road, Exeter EX4 4QD, U.K., Department of Structural Chemistry, Biovitrum AB, SE 112 76 Stockholm, Sweden, Department of Chemistry, University of Sheffield, Sheffield S3 7HF, U.K., Department of Chemistry and Biochemistry, University of Arkansas, Fayetteville, Arkansas 72701, Department of Chemistry, University of Miami, Coral Gables, Florida 33124, and Department of Physics, AlbaNova University Center, Stockholm's Center for Physics, Astronomy and Biotechnology, SE 106 91 Stockholm, Sweden

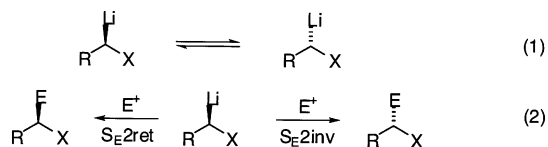
Received April 2, 2004; E-mail: i.coldham@sheffield.ac.uk; bgawley@uark.edu; haeffner@physto.se

Abstract: Kinetics experiments have been used to establish the free energy, enthalpy, and entropy of activation for the enantiomerization of three structural classes of 2-lithiopyrrolidines. We find that α -aminoorganolithiums chelated by a *N*-methoxyethyl or *N*-Boc group have a barrier to enantiomerization (ΔG^\ddagger) 2–3 kcal/mol lower than that of unstabilized α -aminoorganolithiums at 273 K. Density functional calculations were performed to clarify possible ground state and transition structures and to identify possible pathways for inversion of these chiral organolithium species.

The recent appearance of three review monographs attests to the unparalleled importance of organolithium species as the most widely used class of organometallic reagents in organic synthesis.¹ Central to the explosive growth of this field over the last 20 years is the use of chiral, nonracemic organolithiums in asymmetric synthesis. Many new methods employ organolithiums in which the metal-bearing carbon atom is stereogenic and also possesses a heteroatom ligand (X in eq 1). Many chiral organolithium species are versatile in asymmetric synthesis due to their configurational stability and their ability to form carbon–carbon bonds, often with a high degree of stereoselectivity.² For example, dipole-stabilized α -aminoorganolithiums, “unstabilized” *N*-methyl-2-lithiopyrrolidines and piperidines, α -oxy-, and α -thioorganolithiums have been demonstrated to resist inversion particularly at low temperatures, such as -78°C , and in some cases to have configurational stability at or near room temperature. On the other hand, several (especially benzylic) chiral organolithiums can be dynamically resolved by electrophilic substitution in the presence of a chiral ligand.³ Despite significant interest in these compounds, little is known

about the dynamics of inversion or the factors that facilitate dynamic resolution.

Successful use of carbanionic stereocenters for asymmetric synthesis relies on several factors. One is the configurational stability/lability of the carbanionic carbon (eq 1), and another is the steric course of their reaction, such as electrophilic substitution, which may occur with either retention or inversion of configuration (eq 2; electrophile depicted as E^+).⁴ Obviously, the relative rates of these processes affect the steric course of a reaction.



Hoffmann introduced a test based on kinetic resolution of racemic organolithiums, which may be used to evaluate configurational stability on a time scale *relative* to the rate of reaction with a chiral electrophile.⁵ A variant of this test was introduced by Beak and relies on *unequal* amounts of organolithium enantiomers complexed to the chiral ligand, (–)-sparteine.⁶ While these kinetic tests are useful, they do not supply fundamental information on the barrier to inversion of chiral, nonracemic organolithium compounds or the mechanism by which they invert.

In some cases, dynamic NMR spectroscopy may be used to evaluate barriers using coalescence phenomena resulting from

[†] University of Exeter.

[‡] Biovitrum AB.

[§] University of Sheffield.

[¶] University of Arkansas.

[#] University of Miami.

[@] Stockholm's Center for Physics, Astronomy and Biotechnology.

(1) (a) Clayden, J. *Organolithiums: Selectivity for Synthesis*; Pergamon: New York, 2002. (b) Hodgson, D. M., Ed. *Organolithiums in Enantioselective Synthesis*; Springer-Verlag: Heidelberg, Germany, 2003. (c) Rappoport, Z.; Marek, I., Eds. *The Chemistry of Organolithium Compounds*; Wiley: New York, 2004.

(2) Basu, A.; Thayumanavan, S. *Angew. Chem., Int. Ed.* **2002**, *41*, 716–738.

(3) Beak, P.; Anderson, D. R.; Curtis, M. D.; Laumer, J. M.; Pippel, D. J.; Weisenburger, G. A. *Acc. Chem. Res.* **2000**, *33*, 715–727.

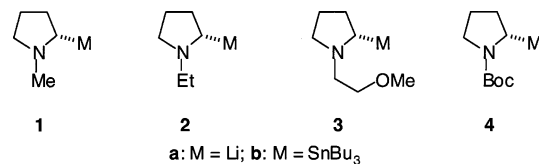
(4) Gawley, R. E. *Tetrahedron Lett.* **1999**, *40*, 4297–4300.

(5) Hirsch, R.; Hoffmann, R. W. *Chem. Ber.* **1992**, *125*, 975–982.

(6) Basu, A.; Gallagher, D. J.; Beak, P. *J. Org. Chem.* **1996**, *61*, 5718–5719.

enantiomerization of racemic organolithiums,^{7,8} but such studies are limited to inversions having free energy barriers (ΔG^\ddagger) sufficiently low that coalescence may be observed on the NMR time scale, at temperatures where the organolithium is chemically stable. Alternatively, an enantioenriched organolithium may be generated by metal exchange, aged, and then quenched with an electrophile to reveal the enantiomer ratio (er) after a specific time interval. This method is valid if both the exchange reaction and the electrophilic quench are stereospecific, and it is applicable to organolithiums that have sufficiently high barriers to inversion and are not amenable to the DNMR approach.

A particularly useful class of organolithiums with broad versatility as reagents is that with a nitrogen atom at the α -position.⁹ Among this class of compounds, 2-lithiopyrrolidines possess a widely diverse set of reactivities in electrophilic substitutions^{10–13} (some of which are mediated by transition metals¹⁴), sigmatropic rearrangements,¹⁵ anionic cyclizations,^{16,17} and dynamic resolutions.¹⁸ In light of the broad usefulness of 2-lithiopyrrolidines, we have investigated the kinetics of enantiomerization of **1a–4a**. These compounds are representative of three structural classes that have differing reactivities and differing chemical and configurational stabilities. Unstabilized species, such as **1a** and **2a**, exhibit excellent reactivity toward numerous electrophiles^{13,18} while exhibiting extraordinary configurational stability (for hours at ≤ -40 °C).¹⁹ The chelated, but unstabilized, species **3a** is somewhat less stable configurationally, resisting racemization only at temperatures below -60 °C.¹⁹ The dipole-stabilized species **4a** also exhibits significant configurational stability¹¹ but has not been quantitatively compared to the other two classes prior to this work.



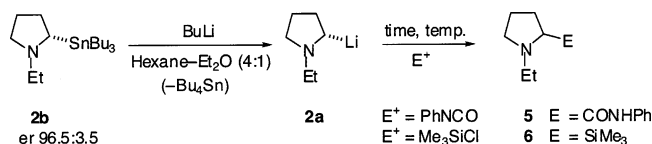
Note the distinction between the terms enantiomerization and racemization. Enantiomerization is the conversion of one enantiomer to another, whereas racemization describes the conversion of an enantioenriched substance to a racemate. As equilibrium is approached, the rate of racemization falls to zero, even if the rate of enantiomerization is fast. In both processes, the initial rate of disappearance of the major enantiomer is the same ($-d[S]/dt$). However, the initial rate of appearance of the racemate is twice the rate of enantiomerization since enantiomerization of one *S* makes one *R*, which pairs with an unreacted *S* to give one (*S,R*) racemate (i.e., $d[SR]/dt = 2 \cdot d[R]/dt = -2 \cdot d[S]/dt$).

Results

Pyrrolidine **4b** was prepared by asymmetric deprotonation of *N*-Boc-pyrrolidine and by addition of tributyltin chloride according to the method of Beak.^{10,11} Pyrrolidine **1b** was prepared by DIBAL-H reduction of **4b**, whereas **2b** and **3b** were prepared by removal of the Boc group, acylation, and reduction.¹⁹ Tin–lithium exchange was effected at various temperatures in THF, Et₂O, or in a mixture of hexane and Et₂O (4:1) using *n*-butyllithium. After the er of the stannanes was determined under conditions at which enantiomerization is negligible, the kinetics of enantiomerization were carried out as summarized below. For details, see the Supporting Information. Density functional calculations were performed to identify ground states, transition states, and intermediates for enantiomerization, taking into account the aggregation state (if known).

***N*-Ethyl-2-lithiopyrrolidine 2a.** Since the *N*-ethyl derivative **2b** was slightly easier to prepare than the corresponding *N*-methyl derivative **1b** and product **5** was easier to analyze for its enantiomer ratio, kinetic experiments were conducted with **2a** as a representative unstabilized and unchelated 2-lithiopyrrolidine (Scheme 1). Treatment of stannane **2b** with *n*-

Scheme 1



butyllithium in hexanes–Et₂O (4:1) at 19 °C and by allowing the mixture to age for 10–45 min, followed by cooling and quenching with phenylisocyanate or trimethylsilyl chloride (TMSCl), gave products **5** and **6**. In all cases, complete transmetalation occurred (as determined by the recovery of tetrabutyltin), although transmetalation required at least a few minutes at room temperature in this solvent system. The enantiomer ratios of **5** were determined using chiral HPLC (chiralpak AD column, see Supporting Information for more detail). Enantiomer ratios of product **6** were determined by ¹H NMR spectroscopic analysis in the presence of (*R*)-(–)-2,2,2-trifluoro-1-(9-anthryl)ethanol. A logarithmic plot of concentra-

- (7) (a) Reich, H. J.; Dykstra, R. R. *Angew. Chem., Int. Ed. Engl.* **1993**, *32*, 1469–1470. (b) Reich, H. J.; Kulicke, K. J. *J. Am. Chem. Soc.* **1995**, *117*, 6621–6622. (c) Gaul, C.; Arvidsson, P. I.; Bauer, W.; Gawley, R. E.; Seebach, D. *Chem.–Eur. J.* **2001**, *7*, 4117–4125.
- (8) Ahlbrecht, H.; Harbach, J.; Hoffmann, R. W.; Ruhland, T. *Liebigs Ann. Chem.* **1995**, 211–216.
- (9) Gawley, R. E.; Coldham, I. In *The Chemistry of Organolithium Compounds (Patai Series)*; Rappoport, Z., Marek, I., Eds.; Wiley: Chichester, U.K., 2004; pp 997–1053.
- (10) Kerrick, S. T.; Beak, P. *J. Am. Chem. Soc.* **1991**, *113*, 9708–9710.
- (11) (a) Beak, P.; Kerrick, S. T.; Wu, S.; Chu, J. *J. Am. Chem. Soc.* **1994**, *116*, 3231–3239. (b) Bertini Gross, K. M.; Beak, P. *J. Am. Chem. Soc.* **2001**, *123*, 315–321.
- (12) (a) Nikolic, N. A.; Beak, P. In *Organic Syntheses*; Freeman, J. P., Ed.; Wiley: New York, 1998; Coll. Vol. 9, pp 391–396. (b) Gawley, R. E.; Campagna, S. In *ECHE96: Electronic Conference on Heterocyclic Chemistry*; Rzepa, H., Snyder, J., Eds.; Royal Society of Chemistry (www.ch.ic.ac.uk/ectoc/echet96).
- (13) (a) Gawley, R. E.; Zhang, Q. *J. Am. Chem. Soc.* **1993**, *115*, 7515–7516. (b) Gawley, R. E.; Zhang, Q. *J. Org. Chem.* **1995**, *60*, 5763–5769.
- (14) (a) Dieter, R. K.; Dieter, J. W.; Alexander, C. W.; Bhinderwala, N. S. *J. Org. Chem.* **1996**, *61*, 2930–2931. (b) Dieter, R. K.; Li, S. *J. Org. Chem.* **1997**, *62*, 7726–7735. (c) Dieter, R. K.; Lu, K.; Velu, S. E. *J. Org. Chem.* **2000**, *65*, 8715–8724. (d) Dieter, R. K.; Alexander, C. W.; Nice, L. E. *Tetrahedron* **2000**, *56*, 2767–2778. (e) Dieter, R. K.; Topping, C. M.; Nice, L. E. *J. Org. Chem.* **2001**, *66*, 2302–2311. (f) Dieter, R. K.; Topping, C. M.; Chandupatla, K. R.; Lu, K. *J. Am. Chem. Soc.* **2001**, *123*, 5132–5133.
- (15) Gawley, R. E.; Zhang, Q.; Campagna, S. *J. Am. Chem. Soc.* **1995**, *117*, 11817–11818.
- (16) (a) Coldham, I.; Hufton, R.; Snowden, D. J. *J. Am. Chem. Soc.* **1996**, *118*, 5322–5323. (b) Coldham, I.; Fernández, J.; Price, K. N.; Snowden, D. J. *J. Org. Chem.* **2000**, *65*, 3788–3795. (c) Coldham, I.; Vennall, G. P. *Chem. Commun.* **2000**, 1569–1570. (d) Coldham, I.; Hufton, R.; Price, K. N.; Rathmell, R. E.; Snowden, D. G.; Vennall, G. P. *Synthesis* **2001**, 1523–1531.
- (17) Ashweek, N. J.; Coldham, I.; Snowden, D. J.; Vennall, G. P. *Chem.–Eur. J.* **2002**, *8*, 195–207.
- (18) Coldham, I.; Dufour, S.; Haxell, T. F. N.; Howard, S.; Vennall, G. P. *Angew. Chem., Int. Ed.* **2002**, *41*, 3887–3889.
- (19) (a) Gawley, R. E.; Zhang, Q. *Tetrahedron* **1994**, *50*, 6077–6088. (b) Gawley, R. E.; Narayan, S.; Vivic, D. A. *J. Org. Chem.* published online Nov. 20, 2004 <http://dx.doi.org/10.1021/jo048569w>.

Table 1. Summary of Activation Parameters for Enantiomerization of **2a** in 4:1 Hexanes–Et₂O

ΔH^\ddagger (kcal/mol)	ΔS^\ddagger (cal/K·mol)	ΔG^\ddagger (kcal/mol)			
		276 K (3 °C)	283 K (10 °C)	292 K (19 °C)	301 K (28 °C)
22 (±1)	+1 (±3)	22 (±1)	22 (±1)	22 (±1)	22 (±1)

tion over time (see Supporting Information for derivations and graphs) gave a straight line, consistent with first-order kinetics. Doubling the concentration from 0.09 to 0.18 M caused the initial rate of enantiomerization to increase from approximately 2×10^{-5} to 4.5×10^{-5} mol/L·s, consistent with a first-order process.

The thermodynamic parameters for the enantiomerization were determined by measuring the first-order rate constants at four different temperatures. These data are detailed in the Supporting Information. In each case, the data correlate well to a first-order process. An Eyring plot (see Supporting Information) revealed the activation parameters, as summarized in Table 1.

The hexanes–Et₂O solvent system is suitable for this study since transmetalation (which requires at least some Et₂O) occurs at a rate that does not significantly interfere with the kinetic measurements and organolithium **2a** is chemically stable for prolonged periods even at room temperature. With THF as the solvent, transmetalation is rapid at a low temperature, even at –78 °C. No kinetic measurements for enantiomerization can be carried out as no racemization takes place; after several hours at a low temperature or when warmed to about –20 °C, decomposition occurs.

In an attempt to determine any influence of an additive on the rate of enantiomerization, stannane **2b** (er = 95:5) was treated with *n*-butyllithium in THF at –40 °C to give the organolithium species, **2a**. Quenching the mixture in the absence of an additive after 35 min with TMSCl gave product **6** (73% yield, er ~ 95:5). This result follows that expected based on the known configurational stability of **1a** at a low temperature (although note that TMEDA was not required for chemical stability).¹⁹ Addition of hexamethylphosphoramide (HMPA) to the mixture immediately after addition of the butyllithium caused decomposition, and none of product **6** was isolated after the TMSCl quench. However, addition of 1 equiv of *N,N,N',N',N''*-pentamethyldiethylenetriamine (PMDTA), followed after 35 min at –40 °C by TMSCl, gave **6** in 73% yield and an er of 77:23. This is in contrast to **1a**·TMEDA, which is configurationally stable for 45 min at –40 °C.¹⁹

DFT Calculations on Monomeric and Dimeric *N*-Methyl-2-lithiopyrrolidine **1a.** To gain more information on the relative energies and structures of the organolithium species and their transition states, density functional theory calculations were carried out. A ground state of the monomer of (*S*)-*N*-methyl-2-lithiopyrrolidine **1a** was computed in which the Li⁺ cation coordinates both the carbanion and the nitrogen atom, consistent with spectroscopic evidence of coordination to nitrogen in lithiopyrrolidines.²⁰ The solvent THF was modeled by two dimethyl ether molecules coordinating to Li⁺. Note that both the metal-bearing carbon and the nitrogen are stereogenic, and both must be inverted to achieve enantiomerization. From the

geometry-optimized ground state, a transition structure (TS1) in which the carbanion center inverts was located and its geometry optimized. The structures are presented in Figure 1. After zero-point correction, the metal-bearing carbon was computed to invert with a barrier of 15.2 kcal/mol. After passing through the transition state, an intermediate structure was found and optimized. Note the inversion of the carbon but not the nitrogen atom in the intermediate. The intermediate was computed to be 1.9 kcal/mol higher in energy than the ground state. From this intermediate, a transition state (TS2) was located in which the nitrogen inverts and completes the enantiomerization of **1a** (see Figure 1). The activation energy of nitrogen inversion relative to that of the intermediate was computed to be 8.8 kcal/mol.

Previous ⁶Li and ¹³C NMR studies established that *N*-methyl-2-lithiopyrrolidine **1a** exists as a homochiral dimer in the solvent THF, with only one type of ⁶Li.²⁰ These data were used to construct a starting structure of the homochiral dimer of pyrrolidine **1a** with the (*S*) configuration at both carbanion and nitrogen centers. The structure was solvated with a molecule of Me₂O coordinating to each of the two lithium ions. It was then subjected to geometry optimization. The optimized ground-state structure is shown in Figure 2. From this ground state, a transition structure, where one of the carbanion centers inverts, was located. Geometry optimization indicated an activation barrier of 26.1 kcal/mol. The transition structure is shown in Figure 2. An intermediate was found in which one of the carbanion centers had inverted but not the α-nitrogen. The intermediate structure was computed to be 7.8 kcal/mol higher in energy than the ground state. Inversion of the nitrogen center via a second transition state (TS2), with a computed energy barrier of 17.7 kcal/mol relative to that of the ground state, affords a heterochiral dimer. This species has not been observed spectroscopically but might continue by a similar pair of inversions to the homochiral dimer, dissociate to a monomer, or disproportionate to a homochiral dimer. These possibilities have not been pursued computationally.

***N*-Methoxyethyl-2-lithiopyrrolidine **3a**.** The unstabilized organolithium **3a** was prepared from stannane **3b** using *n*-butyllithium in hexanes–Et₂O (4:1). At room temperature, product **7** was found to be racemic even after only 10 min, as judged by quenching with trimethylsilyl chloride (TMSCl) and spectroscopically analyzing the ¹H NMR spectrum in the presence of (*R*)-(-)-2,2,2-trifluoro-1-(9-anthryl)ethanol. At lower temperatures, enantiomerization was sufficiently slow to allow kinetic experiments, and transmetalation is complete in <1 min with this substrate. Organolithium **3a** was formed at four different temperatures and aged over different time periods. Rapid cooling and quenching with TMSCl gave product **7**, the enantiomer ratios of which were determined by CSP–GC (β-Dex 120 column; see Supporting Information). Log plots versus time gave straight lines, suggesting first-order kinetics (see Supporting Information). The initial rate of enantiomerization at 0 °C increased from 6.5×10^{-5} mol/L·s at 0.12 M to 17×10^{-5} mol/L·s at 0.24 M. The observed first-order rate constants at 0 °C and at four concentrations (0.03–0.24 M) varied from

(20) (a) Low, E.; Gawley, R. E. *J. Am. Chem. Soc.* **2000**, *122*, 9562–9563. (b) Gawley, R. E.; Klein, R.; Ashweek, N.; Coldham, I. *Tetrahedron* **2004**, in press.

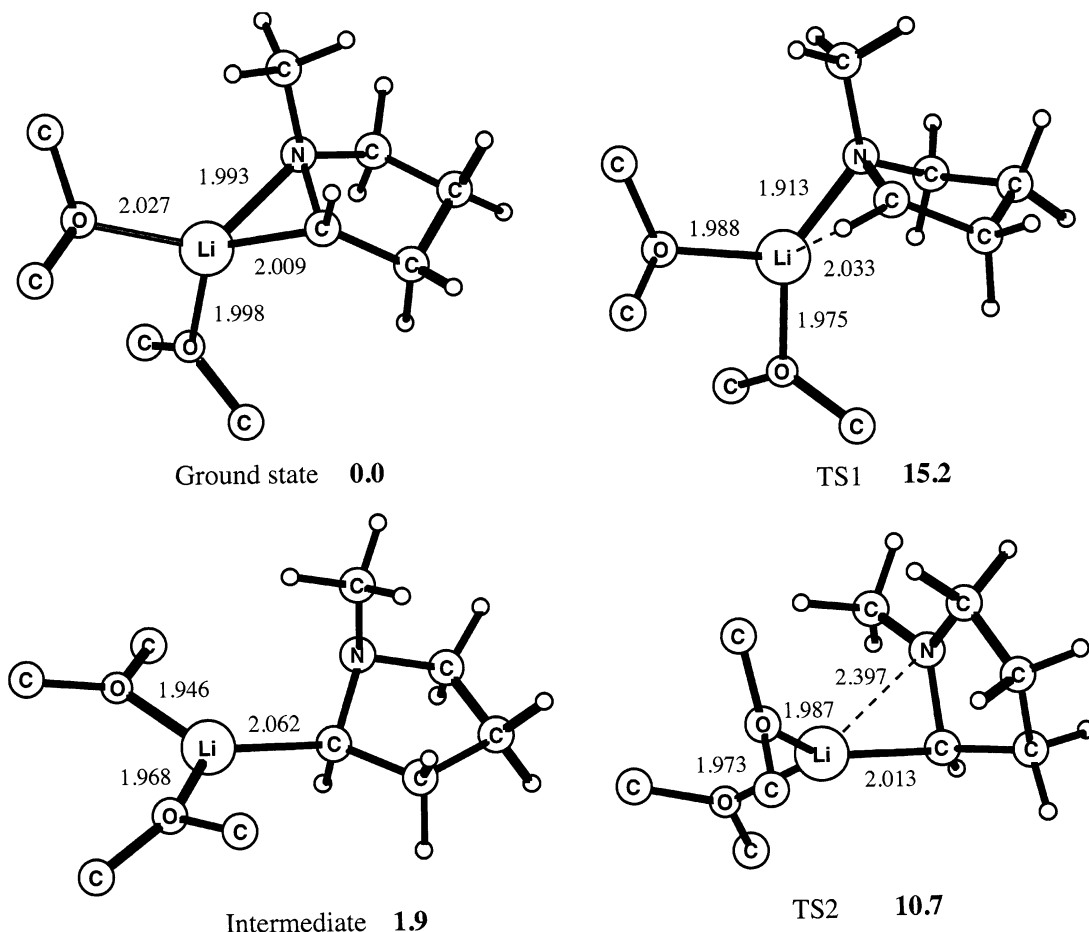


Figure 1. Computed stationary-point structures and energies (kcal/mol) of Me₂O-solvated monomeric **1a**. The structures were geometry-optimized with B3LYP/6-31+G*, and zero-point energies are included. Relative energies in bold are given in kilocalories/mole, and selected bond lengths are presented in angstroms. Hydrogen atoms of the solvent molecules are omitted in the figures for clarity.

Table 2. Summary of Activation Parameters for Enantiomerization of **3a** in 4:1 Hexanes–Et₂O, Assuming First Order

ΔH^\ddagger (kcal/mol)	ΔS^\ddagger (cal/K·mol)	ΔG^\ddagger (kcal/mol)			
		265 K (−8 °C)	273 K (0 °C)	283 K (10 °C)	293 K (20 °C)
20.5 (±3)	+2 (±11)	20 (±3)	20 (±3)	20 (±3)	20 (±3)

Table 3. Summary of Activation Parameters for Enantiomerization of **3a** in THF

ΔH^\ddagger (kcal/mol)	ΔS^\ddagger (cal/K·mol)	ΔG^\ddagger (kcal/mol)			
		248 K (−25 °C)	257 K (−16 °C)	264 K (−9 °C)	273 K (0 °C)
18.5 (±3)	−4 (±10)	19.5 (±3)	20 (±3)	20 (±3)	19.5 (±3)

1.0×10^{-4} to $13.2 \times 10^{-4} \text{ s}^{-1}$. The activation parameters for enantiomerization of **3a** in hexanes–Et₂O are given in Table 2.

The rate of enantiomerization of **3a** in THF was measured. Stannane **3b** was treated with *n*-BuLi in THF at four different temperatures, and the resulting organolithium, **3a**, was aged for 1–180 min before being cooled and quenched with TMSCl. The enantiomer ratios of product **7** were determined by CSP–GC (β -Dex 120 column; see Supporting Information). In this solvent, the enantiomerization followed clean first-order kinetics. The initial rates at -9°C increased from 5.0×10^{-5} to $10.3 \times 10^{-5} \text{ mol/L}\cdot\text{s}$ upon doubling the concentration from 0.19 to 0.38 M; the overall rate constants (k_{obs}) were 2.0×10^{-4} and $2.4 \times 10^{-4} \text{ s}^{-1}$. Eyring analysis (see Supporting Information) yielded the activation parameters listed in Table 3.

To test whether the solvent was involved in the enantiomerization, first-order rates of enantiomerization were measured in 0.2, 0.4, and 0.8 M THF in hexane. A plot of $\ln(k_{\text{obs}})$ versus $\ln[\text{THF}]$ gave a line of near zero slope, indicating that the

enantiomerization of **3a** in hexane is zero order in THF. See the Supporting Information for details.

DFT Calculations on Monomeric *N*-Methoxyethyl-2-lithio-pyrrolidine. Calculations were conducted assuming that *N*-methoxyethyl-2-lithio-pyrrolidine **3a** coordinates the lithium ion with both the nitrogen and the oxygen atoms, leaving only one coordination site open for one Me₂O molecule to complete a tetrahedral first solvation shell around the Li⁺ cation. This complex was subjected to energy minimization and served as the ground state for the inversion of the monomeric form of **3a**. The carbanion of the optimized ground state has the (*S*) configuration, and the nitrogen is (*R*). The geometry-optimized structure is presented in Figure 3. A transition structure was located and optimized in which the carbanion center inverts. The activation energy of this step was computed to 16.6 kcal/mol. After inversion of the carbanion center, an intermediate forms, with an energy 5.3 kcal/mol higher than that of the ground state, followed by a second transition state (TS2), in

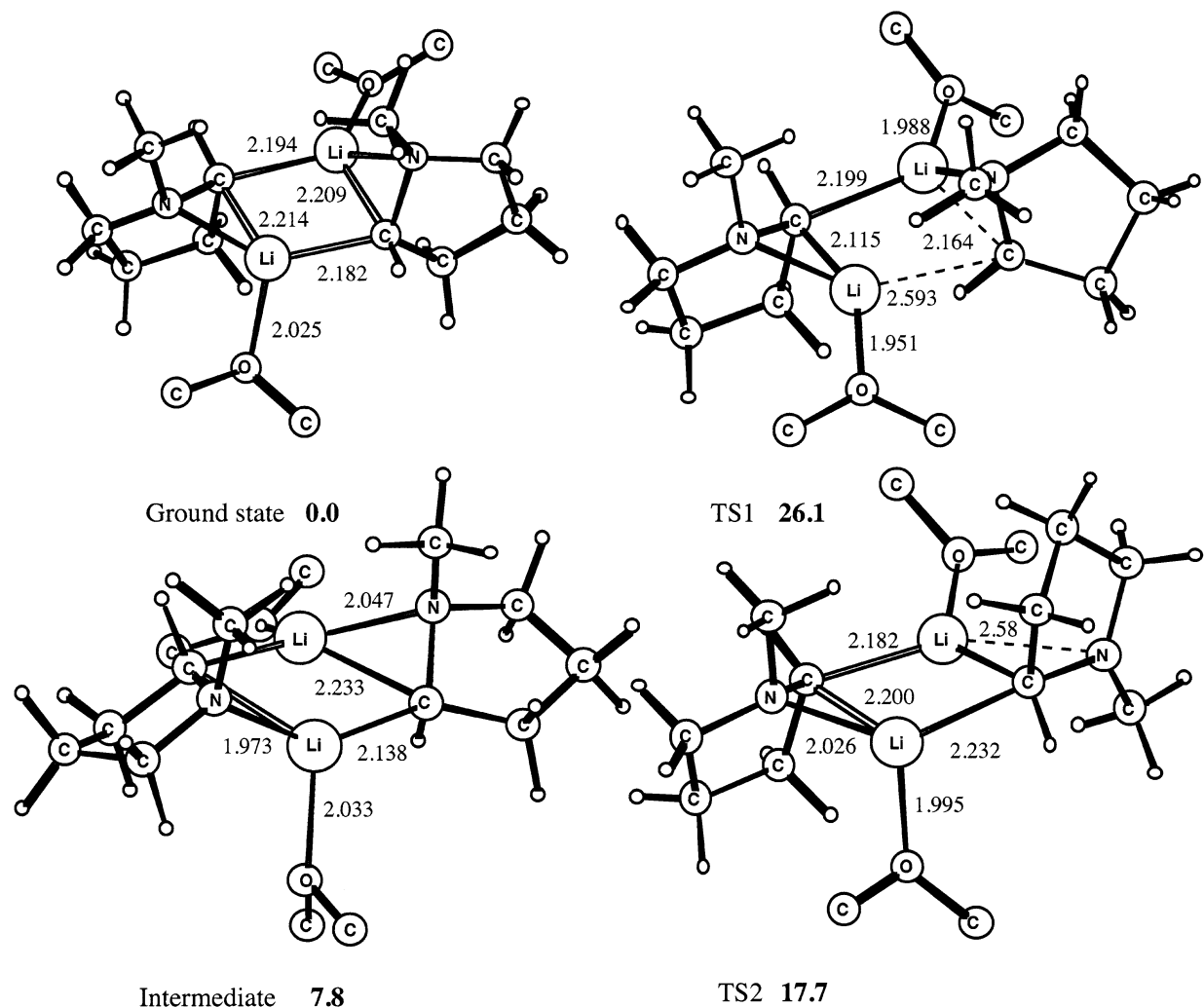


Figure 2. Computed stationary-point structures and energies (kcal/mol) of Me₂O-solvated dimeric **1a**. The structures were geometry-optimized with B3LYP/6-31+G*, and zero-point energies are included. Relative energies in bold are given in kilocalories/mole, and selected bond lengths are presented in angstroms. Hydrogen atoms of the solvent molecules are omitted in the figures for clarity.

which the nitrogen center inverts with a barrier of 6.3 kcal/mol relative to that of the ground state (see Figure 3).

We also studied the inversion of a dimeric aggregate computationally. Consequently, a dimeric ground-state structure and a transition-state structure were also geometry optimized (see Supporting Information). The computed barrier to carbanion inversion was 26.5 kcal/mol. We did not investigate the inversion of the nitrogen center as the rate-limiting step of the dimeric **1a** is the carbanion center inversion, and it is likely that dimeric inversion of **1a** and **3a** follows a similar mechanism with the same rate-limiting step.

N-Boc-2-lithiopyrrolidine 4a. Enantioenriched *N*-Boc-2-lithiopyrrolidine **4a** was synthesized from enantioenriched *N*-Boc-2-tributylstannylpyrrolidine^{10,11} by transmetalation using *n*-BuLi in Et₂O or hexanes–Et₂O (4:1) at –78 °C. The formation of tetrabutylstannane was observed by NMR to be complete within 20 s. Enantiomerization of enantioenriched **4a** was followed by transferring the reaction vessels to baths maintained at constant temperatures (measured internally) and by aging the solutions before quenching with TMSCl. Tetrabutyltin was separated from the products by radial chromatography, and the enantiomeric purity of the resulting silanes was

Table 4. Summary of Activation Parameters for Enantiomerization of **4a**

solvent	ΔH^\ddagger (kcal/mol)	ΔS^\ddagger (cal/K·mol)	ΔG^\ddagger (kcal/mol)		
			240 K (–33 °C)	247 K (–26 °C)	256 K (–17 °C)
Et ₂ O	29 (±2)	40 (±8)	20 (±3)	19 (±3)	19 (±3)
			251 K (–22 °C)	258 K (–15 °C)	268 K (–5 °C)
4:1 hexane–Et ₂ O	26 (±1)	24 (±4)	20 (±1)	20 (±1)	20 (±1)

determined by chiral stationary phase–gas chromatography (see Supporting Information).

The logarithmic plot of the data is consistent with a first-order dependence of the rate, which was confirmed by a doubling of the initial rate from 1.4×10^{-5} to 2.9×10^{-5} mol/L·s, with a change in initial concentration from 3.26×10^{-2} to 6.52×10^{-2} M in Et₂O. Thermodynamic parameters were determined by measuring the first-order rate constants (see Supporting Information) at three different temperatures in the two solvent systems. The excellent correlation to a first-order rate plot is further support for a first-order dependence on

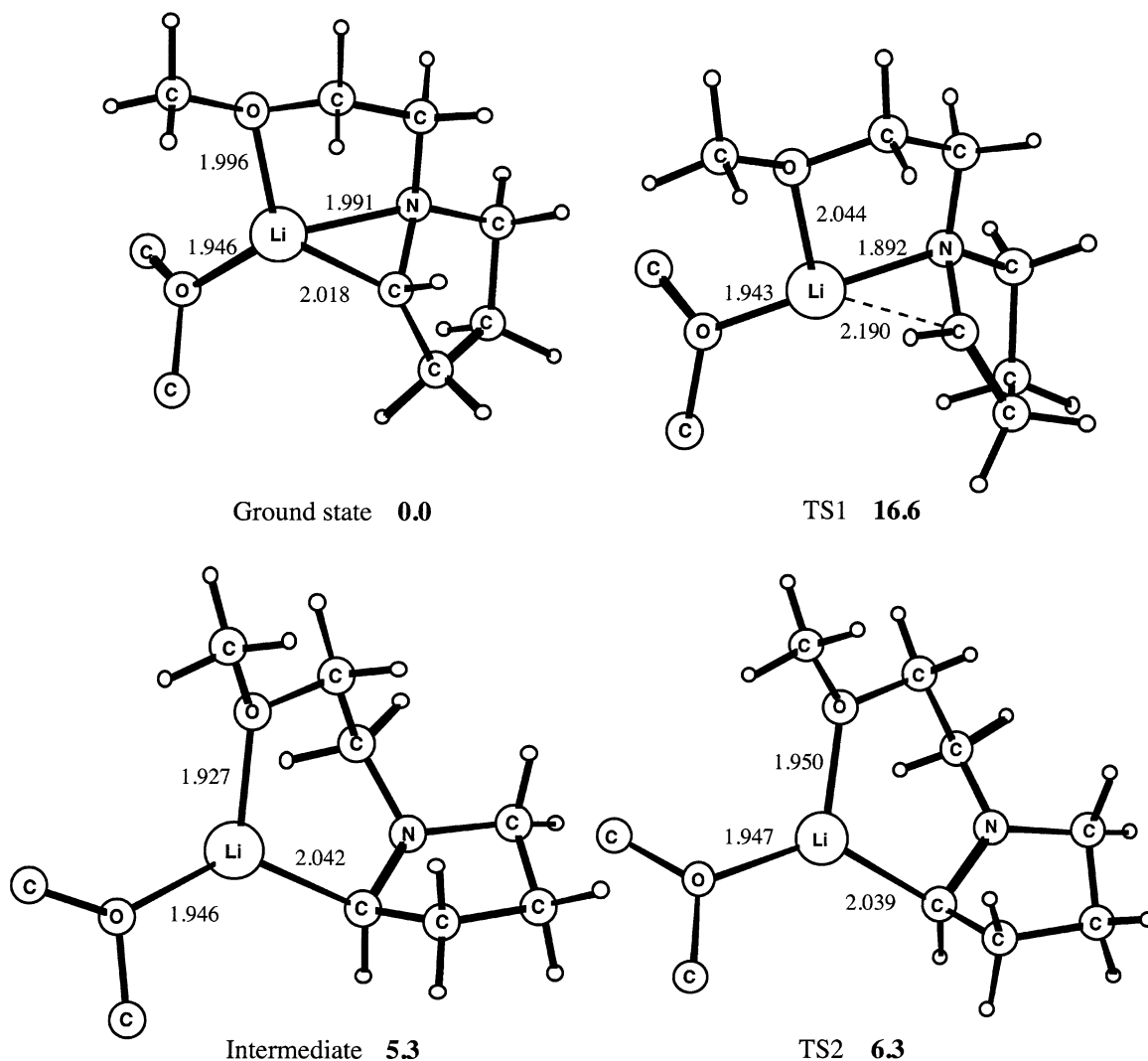


Figure 3. Computed stationary-point structures and energies (kcal/mol) of Me₂O-solvated monomeric **3a**. The structures were geometry-optimized with B3LYP/6-31+G*, and zero-point energies are included. Relative energies in bold are given in kilocalories/mole, and selected bond lengths are presented in angstroms. Hydrogen atoms of the solvent molecules are omitted in the figures for clarity.

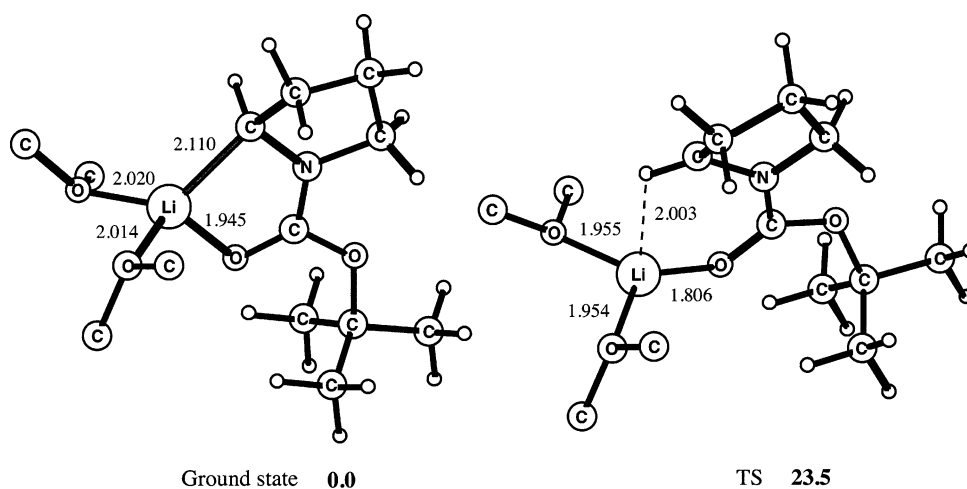


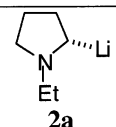
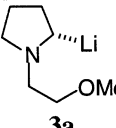
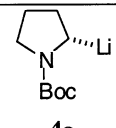
Figure 4. Computed stationary-point structures and energies (kcal/mol) of monomeric **4a**. The structures were geometry-optimized with B3LYP/6-31+G*, and zero-point energies are included. Relative energies in bold are given in kilocalories/mole, and selected bond lengths are presented in angstroms. Hydrogen atoms of the solvent molecules are omitted in the figures for clarity.

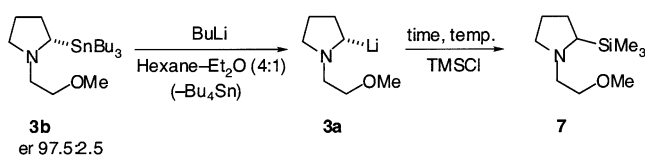
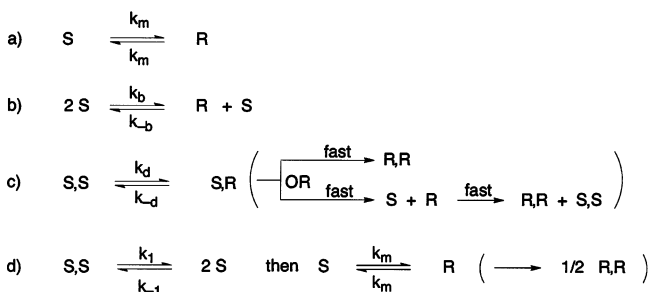
organolithium. Eyring plots revealed the activation parameters, as summarized in Table 4.

DFT Calculations on Monomeric *N*-Boc-2-lithiopyrrolidine. A ground state and a transition state of monomeric *N*-Boc-

2-lithiopyrrolidine **4a** solvated with two molecules of Me₂O were subjected to geometry optimization, and the resulting geometries are presented in Figure 4. The activation energy of the inversion of the carbanion center was computed to be 23.5

Table 5. Summary of Barriers to Inversion of 2-Lithiopyrrolidines

	Solvent	ΔG^\ddagger kcal/mol (273 K)	ΔH^\ddagger kcal/mol	ΔS^\ddagger cal/K·mol	DFT E_a kcal/mol
 2a	4:1 hexane/Et ₂ O	22 (±1)	22 (±1)	1 (±3)	15.2 ^a (monomer) 26.1 ^a (dimer)
 3a	4:1 hexane/Et ₂ O THF	20 (±3) 20 (±3)	20.5 (±3) 18.5 (±3)	2 (±11) −4 (±10)	16.6 (monomer) 26.5 (dimer)
 4a	4:1 hexane/Et ₂ O Et ₂ O	20 (±1) 19 (±3)	26 (±1) 29 (±2)	24 (±4) 40 (±8)	23.5 (monomer)

^a Calculated for **1a**.**Scheme 2****Scheme 3^a**^a *S* and *R* refer to the configuration of the carbanionic carbon. *S* is the monomer and *S,S* is the dimer.

kcal/mol. The inversion of **4a** was found to be concerted, and consequently, passage of the transition state completes the inversion of monomeric **4a**.

Discussion

There are a number of possible mechanisms for enantiomerization of these organolithiums (Scheme 3). Enantiomerization of a monomer could follow first-order kinetics (rate constant k_m , Scheme 3a). Inversion of a monomer via a dimeric transition state would follow second-order kinetics (rate constant k_b , Scheme 3b). Inversion of a dimer could occur by conversion of the homochiral (*S,S*)-dimer to the heterochiral (*S,R*)-dimer, which would follow apparent first-order kinetics (rate constant k_d , Scheme 3c). Alternatively, dissociation of the (*S,S*)-dimer to the monomer could take place (rate constant k_1), followed by inversion (rate constant k_m) and recombination (Scheme 3d).

In this latter case, either dissociation of the dimer or inversion of the monomer could be rate determining. If dissociation of the dimer is rate determining, first-order kinetics would be expected. In principle, any of these steps could be reversible.

Note that these enantiomerization studies are limited in one important way: the temperature range in which the organolithium is chemically stable but configurationally unstable is rather narrow. The kinetics of enantiomerization of chiral organolithium compounds are clearly dependent on a number of factors, not least being the nature of the species present in solution. Note that we have not explicitly determined the concentration of organolithium species in solution; rather, we infer the concentration from that of the stannane precursor, and express it as concentration of monomeric organolithium. Table 5 summarizes the experimental and computational data.

The DFT calculations suggest that the lowest inversion barriers are achieved via monomeric transition states. In all cases studied, the data show first-order kinetics, which eliminates a bimolecular enantiomerization (Scheme 3b). First-order kinetics are also supported by the observation that the initial rates double upon doubling the concentration. On the other hand, comparison of observed rate constants at different concentrations does not show good agreement in some cases. However, there may be good reasons for this, particularly where there may be more than one organolithium species in solution. When the concentration of starting stannane (and the amount of butyllithium/hexanes) is changed, the position of the equilibrium between aggregates, and perhaps their rate of interconversion, may be affected by the increased hexane content. The organolithium species studied herein may be monomeric or dimeric. If it is the latter, both homochiral and heterochiral dimers are possible. At $t = 0$, dimers can only be homochiral. If enantiomerization proceeds via a dimer, such as illustrated in Scheme 3c, the fate of the heterochiral dimer may be affected by the increasing concentration of the (*R*) enantiomer as the reaction proceeds, thus affecting k_{obs} .

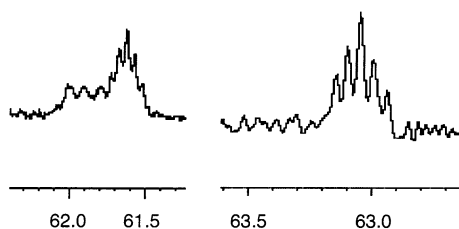


Figure 5. Partial ^{13}C spectrum of $\{^6\text{Li}\}$ -**2a** in $\text{THF-}d_8$, showing the carbanionic carbon (a) in THF and (b) in THF containing pentane.

The Eyring analyses reveal a surprisingly high entropy of activation for **4a** in ether. Eyring plots over small temperature ranges are prone to error since entropy is obtained by extrapolation of $1/T$ to zero (infinite temperature). In the present study, we are limited in the temperature range available since the organolithium compounds decompose at higher temperatures and fail to racemize at lower temperatures. Note that the decomposition of the organolithium over time may introduce some error in the analysis as the kinetic equations implicitly assume that $[\text{RLi}]_{\text{total}}$ is constant. However, the yields do not decrease consistently over time, so the assumption is valid to a first approximation.

Unstabilized Lithiopyrrolidines. For lithiopyrrolidines **1a**–**3a**, coordination of the lithium by the nitrogen atom creates a second stereocenter, each of which must be inverted to complete enantiomerization. The data for the enantiomerization of the *N*-ethyl organolithium **2a** are likely to be similar to those of the *N*-methyl organolithium **1a** and, indeed, of other unstabilized α -aminoorganolithium species. For example, *N*-pent-4-enyl lithiopyrrolidine has a rate constant for enantiomerization at 23 °C in 4:1 hexanes– Et_2O of $k_{\text{obs}} \approx 3.4 \times 10^{-4} \text{ s}^{-1}$.¹⁷ These *N*-alkyl-2-lithiopyrrolidines, lacking other heteroatoms in the nitrogen substituent, have barriers to inversion of approximately 22 kcal/mol at room temperature in hexanes– Et_2O .

NMR studies revealed that the structure of *N*-methyl-2-lithiopyrrolidine **1a** is a homochiral dimer in THF.²⁰ Similar experiments with **2a** afforded surprising evidence of a mixture of species in THF solution (Figure 5a). The triplet at 61.9 ppm, $^1J\{^{13}\text{C}-^6\text{Li}\} = 12 \text{ Hz}$, indicates a single lithium in contact with the carbanionic carbon (probably a monomeric organolithium), while the pentet at 61.6 ppm, $^1J\{^{13}\text{C}-^6\text{Li}\} = 6.0 \text{ Hz}$, is indicative of a dimer. In a solvent mixture containing slightly more hydrocarbon, the signal having only one ^6Li disappears (Figure 5b). Clearly, both monomeric and dimeric unstabilized lithiopyrrolidines are viable in solution. Attempts to use DNMR to investigate the dynamics of the dimer to the monomer interconversion of **2a** were unsuccessful.

The kinetic measurements show that enantiomerization of the unstabilized lithiopyrrolidine **2a** is first order in organolithium, which together with the very low value for the change in entropy is consistent with enantiomerization via either a monomer or a dimer. To complicate matters, both may be present in solution. It is likely that for unstabilized organolithiums **1a** and **2a**, if inversion occurred via a homochiral dimer to a heterochiral dimer (Scheme 3c), the inversion would be followed by rapid decomposition of the heterochiral dimer (*S,R*) to monomers or disproportionation to homochiral dimers. The DFT calculations indicate that the barrier to enantiomerization is lower for the monomer. Indeed, a barrier of only 15.2 kcal/mol was computed for the inversion of the monomer of organolithium **1a**, whereas

the dimer was calculated to invert with a barrier of 26.1 kcal/mol. The computed energy to dissociate the geometry-optimized dimer of **1a** solvated with two molecules of Me_2O into two disolvated monomers is 20.2 kcal/mol [$\text{dimer} \cdot (\text{OMe}_2)_2 + 2 \text{ Me}_2\text{O} \rightarrow 2 \text{ monomer} \cdot (\text{OMe}_2)_2$].

Experiments that may shed some light on the above would be the influence of complexing agents, particularly *N,N,N',N',N'*-pentamethyldiethylenetriamine (PMDTA). The tridentate ligand PMDTA is a strong complexing agent and may occupy three coordination sites of a lithium atom, thereby promoting the formation of monomeric organolithiums.^{21,22} This can influence the configurational stability, and examples are known in which complexation can either reduce or enhance the configurational stability of the resulting organolithium.^{8,19,23} Upon addition of 1 equiv of PMDTA to a THF solution of $\{^6\text{Li}\}$ **2a** produced a new 1:1:1 triplet at 68.8 ppm, indicating a monomer in solution. The addition of 1 equiv of PMDTA to the organolithium **2a** at -40 °C in THF, followed after 35 min by a TMSCl quench, gave product **6** with some loss in enantiopurity (*er* = 77:23). This represents a significant loss of enantiopurity at this temperature, more so than (to our knowledge) any other unchelated, unstabilized α -aminoorganolithium species. This is consistent with a lower inversion barrier via a monomeric transition state. When the concentration of **2a** in 4:1 hexane–ether is doubled, the initial rates double, again consistent with first-order kinetics. On the other hand, the overall k_{obs} changed with a change in concentration. There are subtle effects at play here, which make the comparison of overall rate constants risky, as discussed above. In a hexane–ether solvent, we presume that the predominant structure in solution is a dimer. If the preferred dimeric structure is homochiral, the higher concentration of the enantiomeric monomer may help drain the (*S,S*)/(*S,R*) equilibrium (Scheme 3c), resulting in a larger k_{obs} . In the end, we prefer to compare initial rates, which appear to be the most consistent overall.

Unstabilized, Chelated Lithiopyrrolidines. In the nonpolar solvent mixture of 4:1 hexanes– Et_2O or in THF, enantiomerization of *N*-methoxyethyl-2-lithiopyrrolidine **3a** shows first-order kinetics. NMR spectroscopic studies (data not shown) of $\{^6\text{Li}\}$ **3a** show a predominant species having only one ^6Li on the carbanionic carbon. Unfortunately, this information is not as revealing as one would hope as there are several structures consistent with these data (Figure 6). On the basis of analogy with the *N*-methyl compound **1a** and the corresponding *N*-methylpiperidine,²⁰ the lithium atom may bridge the carbon and nitrogen atoms and/or be coordinated to the ether oxygen atom. Five-membered ring chelation of organolithiums to ethers is known to compete well with solvent coordination.²⁴ More exotic, cyclic dimers, such as **3ad** and **3ae**, are also possible.

A final comment on the enantiomerization of compound **3a**, particularly in the hexanes– Et_2O solvent, relates to the absolute

- (21) Bauer, W. In *Lithium Chemistry: A Theoretical and Experimental Overview*; Schleyer, P. v. R., Sapse, A.-M., Eds.; Wiley: New York, 1995; pp 125–172.
- (22) (a) Lappert, M. F.; Engelhardt, L. M.; Raston, C. L.; White, A. H. *J. Chem. Soc., Chem. Commun.* **1982**, 1323–1324. (b) Bauer, W.; Winchester, W. R.; Schleyer, P. v. R. *Organometallics* **1987**, *6*, 2371–2379. (c) Fraenkel, G.; Chow, A.; Winchester, W. R. *J. Am. Chem. Soc.* **1990**, *112*, 6190–6198.
- (23) (a) Pearson, W. H.; Lindbeck, A. C. *J. Am. Chem. Soc.* **1991**, *113*, 8546–8548. (b) Reich, H. J.; Medina, M. A.; Bowe, M. D. *J. Am. Chem. Soc.* **1992**, *114*, 11003–11004. (c) Chong, J. M.; Park, S. B. *J. Org. Chem.* **1992**, *57*, 2220–2222.
- (24) Reich, H. J.; Goldenberg, W. S.; Sanders, A. W.; Jantzi, K. L.; Tzschucke, C. C. *J. Am. Chem. Soc.* **2003**, *125*, 3509–3521.

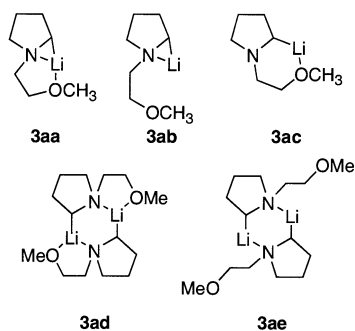


Figure 6. DFT calculations (Figure 3) suggest that the inversion of **3a** is preferable via monomer **3aa** by about 10 kcal/mol when compared to inversion via a dimer. This result, together with the NMR spectroscopy results, is most consistent with a mechanism for inversion of organolithium **3a** via species **3aa**. The change in entropy is close to zero or slightly negative (particularly in THF), although the solvent seems to play no role in the transition state, as indicated by the kinetic studies in hexane–THF that were zero order in THF.

values of the overall rate constants that increase with increasing concentration (see Supporting Information). The enantiomerization appears to be first-order overall, as demonstrated by a number of factors, such as the straight-line log plots, the exponential decay of enantiomeric excess over time, and the approximate doubling of the initial rate when the concentration is doubled. Our assumption is that the k_{obs} value may reflect the presence of more than one species in solution (possibly a monomer and a dimer) and competing mechanisms at different concentrations.

Dipole-Stabilized, Chelated Lithiopyrrolidines. Previous studies¹¹ have shown that **4a** is configurationally stable in ether or THF at -78°C . Racemization occurs at -40°C in ether and is accelerated by TMEDA. We were unable to detect any ^6Li – ^{13}C coupling in the NMR spectrum of **4a**. For the sake of simplicity, we are working under the hypothesis that it is a monomer in solution. Excellent first-order kinetics were observed for the enantiomerization of the *N*-Boc derivative **4a** in hexanes–ether or in ether. At temperatures above -78°C in THF, decomposition is rapid, and enantiomerization could not be studied. Previous DFT calculations on 2-lithio-*N*-formylpyrrolidine (the Boc-group of **4a** was replaced by a formyl group) indicated that this species inverts as a monomer in a solvent, such as dimethyl ether, with a barrier to inversion of 15.7 kcal/mol.²⁵ The calculations above (Figure 4) indicate that the *N*-Boc compound **4a** has a barrier to inversion of 23.5 kcal/mol, a value that is more similar to the enthalpy determined by experiment.

(25) Häffner, F.; Brandt, P.; Gawley, R. E. *Org. Lett.* **2002**, *4*, 2101–2104.

It is therefore apparent that the nature of the substituent on the carbonyl group can have a significant influence on the DFT calculations.²⁶

The large positive entropy of activation for enantiomerization of **4a** stands in stark contrast to the neutral or negative activation entropies of **2a** and **3a**. We hypothesize that because of the large *tert*-butoxy group that must move as the lithium is conducted to the opposite face of the carbon atom, significant solvent reorganization ensues. We have observed a dynamic phenomenon (by NMR) that may be solvent exchange in a related *N*-Boc-2-lithiopyrrolidine.^{20b}

Summary

These studies on unstabilized (alkyl group on nitrogen), unstabilized and chelated (methoxyethyl group on nitrogen), and dipole-stabilized and chelated (Boc group on nitrogen) lithiopyrrolidines reveal free energies for enantiomerization in the range of 19–22 kcal/mol at 0°C . Despite the similarity of these numbers, the enthalpic and entropic contributions to the free energies vary widely and exhibit a marked dependence on solvent.

Acknowledgment. N.J.A. and S.D. are grateful to the EPSRC (U.K.) for funding. The Leverhulme Trust (U.K.) is thanked for support of this work (G.S.-J.). F.H. is grateful to the Knut and Alice Wallenberg foundation for financial support of this research. We thank parallelldatorcentrum (PDC) for supplying computer time, and Dr. J. P. B. Sandall (University of Exeter, U.K.) and Dr. N. H. Williams (University of Sheffield, U.K.) for helpful discussions concerning the kinetics. Work at the University of Miami and at the University of Arkansas was supported by the National Institutes of Health (GM 562701 and P20 R15569) and the Arkansas Biosciences Institute. R.K. is grateful to the University of Miami for a Maytag Fellowship. Collaborative work between the Gawley and Coldham groups was supported by the Leverhulme Trust (U.K.) and the U.S. National Science Foundation (INT 0000096). We are also grateful to the referees for several helpful comments and suggestions.

Supporting Information Available: Experimental and computational details. In addition, kinetic plots for the enantiomerizations of **2a**–**4a**. This material is available free of charge via the Internet at <http://pubs.acs.org>.

JA048090L

(26) Wiberg, K. B.; Bailey, W. F. *J. Org. Chem.* **2002**, *67*, 5365–5368.